Resistance of Punching Shear Strength of RC Flat Slabs According to Laboratory and Finite Element Analysis Study Comparison of International Codes

Hanna F. H. Habeb [1], Ahmed A. Mahmoud*[2], Alaa G. Sherif [3], Magdy M.M. Genidi[4]

*Corresponding author, Tel: 20201005679172, E-mail: ahmed.ahmed@feng.bu.edu.eg, ahmed.m5882@gmail.com

Department of Civil Engineering, Faculty of Engineering at Shoubra, Benha University - , 108 Shoubra Street, Shoubra 11691, Cairo, Egypt.

1- **Higher Institute of Engineering, 15th of May City, Egypt (E-mail: civil.hanafakhry@yahoo.com).**

2- **Professor, Faculty of Engineering (Shoubra), Benha University, Egypt (E-mail: ahmed.ahmed@feng.bu.edu.eg and ahmed.m5882@gmail.com);**

3- **Professor of Reinforced Concrete Structures, Civil Engineering Dept., (Structure), Faculty of Engineering El Matarya- Helwan University, Cairo, Egypt (E-mail: alaa sherif@m-eng.helwan.edu.eg and** agbsherif@gmail.com**);**

4- **Associate Professor, Civil Engineering Dept., (Structure), Faculty of Engineering El Matarya-Helwan University, Cairo, Egypt (E-mail: magdy_genedy@m-eng.helwan.edu.eg   and magdy_genidi@yahoo.com).**

ABSTRAT

The main objective of this paper is to study the effect of the proposed external strengthening techniques to resist punching shear of reinforced concrete flat slabs using nonlinear finite element. The finite element (FE) analysis software program (ANSYS V. 19) was used to create the models and investigate the effects of some parameters on punching shear of reinforced concrete flat slabs. Ten variable parameters are taken into consideration during study full scale flat slab models to account the influence of: (1) concrete compressive strength f_{cu}; (2) reinforcing steel yield strength f_y; (3) slab thickness (t_s); (4) shear studs and stirrups diameter (D_b); (5) shear studs (stirrups) spacing /t_s ratio (S_b/t_s); (6) shear studs stirrups spacing/t_s ratio (D/ t_s); (7) main steel ratio/μ_{max} (μ /μ_{max}); (8) top steel ratio/μ_{max} (μ` /μ_{max}); (9) drop thickness/t_s ratio (t_d/ t_s) and (10) drop diameter/t_s ratio (D_d/ t_s).The numerical results were compared with the analytical results calculated from ECP 203-2017 [1] and ACI 318-19 [2]. The comparison showed a great match between the numerical results and the results of the two codes, especially ACI 318-19 [2].

Keywords: Flat slabs, punching shear, experimental, external strengthening, ANSYS program, numerical analysis, nonlinear finite element, international codes.

1. INTRODUCTION

Flat slab now is one of the most common systems in reinforced concrete structures. It provides architectural flexibility, more clear space, less building height, easier formwork and, consequently shorter construction time. A flat slab floor system using when there is a need for more clear head such as car parks, libraries and multi-story buildings where larger spans are also required.

Punching shear failure is a major problem encountered in the design of reinforced concrete flat slabs. Many researchers have studied the punching shear behavior of reinforced concrete flat slabs [3-6]. The punching shear strength and deformation capacity are strongly influenced by the type and characteristics of the shear reinforcing system [7-13]. The slabs punching shear reinforcing system are: (1) separated stirrups, (2) continuous stirrups, (3) bonded reinforcement with anchorage plates, (4) steel plates, (5) continuous FRP sheets, (6) FRP strips, (7) internal prestressing, (8) external prestressing, (9) bent up bars, (10) vertical studs, and (11) inclined studs.

Failures of flat slab structures were reported during construction and brittle failure happens with no enough warnings [14]. Punching shear is a critical design factor of reinforced concrete flat slabs where it is associated with brittle failure

The experimental results showed that the increase of concrete strength leads to increase of ultimate load of the slab and flat slabs resisting by steel fiber reinforcement have the highest punching shear resistance comparing to its corresponding slabs resisting by added straight bars [15- 16].
There are many researches that talk about external strengthening to resist punching shear [17 -18]. Robbert, K. et al. [17] conducted an experimental study of large-scale reinforced concrete flat slabs crosswise reinforced with carbon fiber reinforced polymer (CFRP) strips against punching shear.

Hamed, S. A. [18] examined retrofitted flat slabs, which were damaged by punching shear using pre-pressing with vertical screws. The comparison between the behavior of the modified slabs and their references showed that the proposed repair system is effective and can be used in practice. The comparison between the experimental results and the punching load failure computed on the basis of formulas adopted by different codes showed reasonable agreement.

2. NONLINEAR FINITE ELEMENT ANALYSIS

In this study, nonlinear structural analysis program ANSYS V19 is used to create numerical simulation. The following steps were taken in order to analyze the considered slabs specimens: (1) selection of element type; (2) assigning material properties; (3) modeling and meshing volume; (4) applying loads and boundary conditions, then solving [26]. Flat slab reinforced concrete was modeled using SOLID65. The reinforcing bars, steel shear studs and GFRP stirrups were idealized using a 2-node bar (linear) named (Link 180). GFRP sheets in the compression side represented by element (Shell 181) as shown in Fig. 1.

The tested slabs discretized using equal-size 3-D isoperimetric elements (25*25*25 mm) Solid 65 as shown in Fig. 2. The column stub was represented as shown in the figure to simulate the actual shape and dimensions of column stub of the tested specimens. The slabs were analyzed as simply supported along the four sides to simulate the experimental set-up.

Referring to ANSYS V19 technical manual [26], the three-dimensional isoparametric element Solid65 was adopted to model the concrete elements. Solid 65 element is capable of cracking in tension and crushing in compression. This element is similar to the one recommended., which introduced a three-dimensional, 8-node isoparametric element.

Solid 65 element is defined by eight nodal points each having three translational degrees of freedom x, y, and z (and no rotational deformations), along with a 2 x 2 x 2 Gaussian integration scheme which is used for the computation of the element stiffness matrix. The element can represent one solid material (concrete), and up to three impeded reinforcing bars with different material properties. Both linear and nonlinear responses of the concrete were included. For the linear stage, the concrete is assumed to be an isotropic material up to cracking. For the nonlinear, the concrete may undergo plasticity. Cracking may take place up to three orthogonal directions at each integration point.

Link180 is a 3-D spar that is useful in a variety of engineering applications. The element can be used to model trusses, sagging cables, links, springs, and so on. The element is a uniaxial tension-compression element with three degrees of freedom at each node: translations in the nodal x, y, and z directions.

Shell 181 is suitable for analyzing thin to moderately-thick shell structures. It is a four-node element with six degrees of freedom at each node: translations in the x, y, and z directions, and rotations about the x, y, and z-axes. The software package "ANSYS V. 19.0" [26] allows steel reinforcement to be defined using the smeared reinforcement approach, in which the amount of reinforcement is defined by specifying a volume ratio and orientation angles of the rebar.
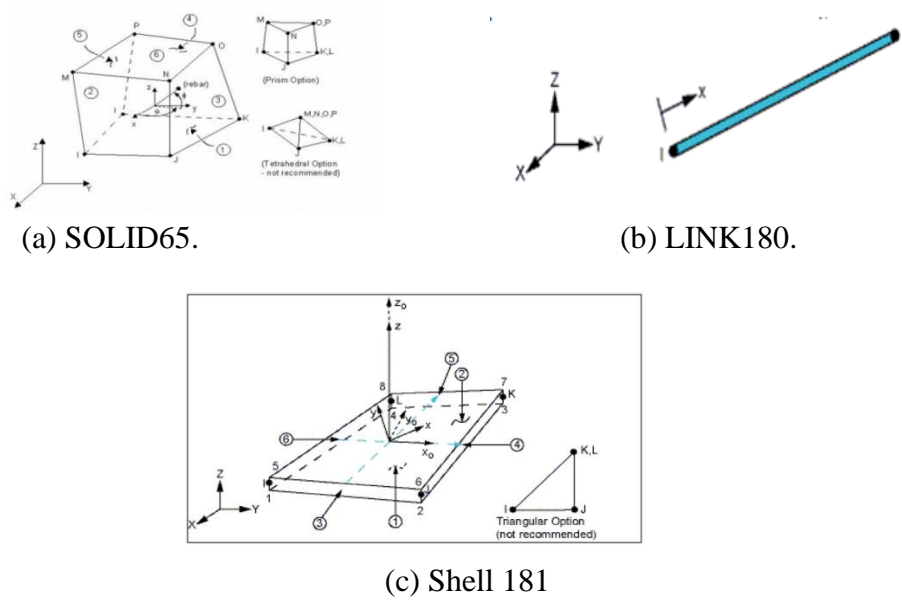
(a) SOLID65.   (b) LINK180.

(c) Shell 181

Fig. 1 Elements Geometry [26].

(a) Concrete elements (Solid 65)   (b) Reinforcing bar elements (Link 180)
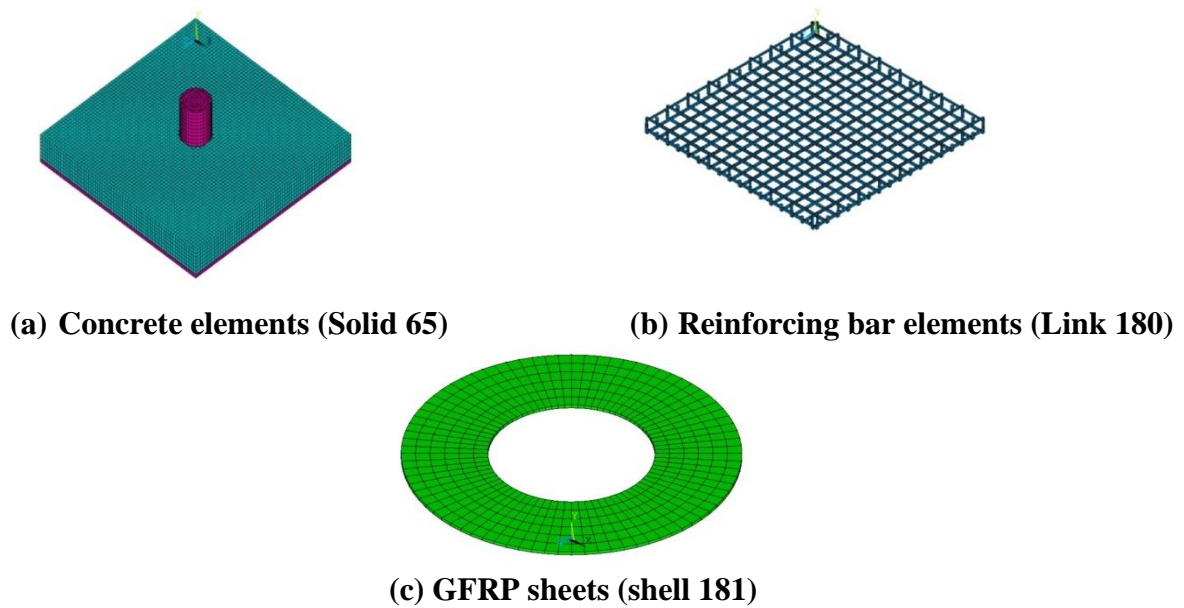

(c) GFRP sheets (shell 181)

Figure 2 ANSYS idealization of the slabs.

3. VERIFICATION and FALIDATION

3.1 Details of studied slabs

One slab from Hanna, F.H.H. [27] (named Sc) was used to verify the numerical and the analytical results. The average cubic and cylindrical concrete compressive

strength were 26 and 22 MPa, respectively. The cracking strength of concrete was taken as 10% of the concrete compressive strength.

A fiberglass is a custom of fiber-reinforced plastic. Usually, the glass fiber is flattened in a sheet, randomly arranged or woven in a fabric. Fiberglass is made from different types of glass according to their use. Fiberglass is strong, less brittle and lightweight. The best advantage fiberglass is its ability to get shaped in different difficult shapes. The glass fibers used to produce the GFRP sheet were sika, which is a product of sika company, and the used polymer was polyester. The Mechanical properties of the used fibers are given - according to the manufacturer in Table 1.

Table 1 Mechanical Properties of GFRP.

Property	GFRP
Fabric design thickness	0.17 mm
Weight / Area	0.445×10^{-5} weight N/mm^2
Tensile strength	1000 MPa
Modulus of elasticity	76000 MPa
Strain at failure	2.80%

The used Epoxy was Sikadur -165 which is also a product of Sika construction company as well. Shear bolts have diameter 16 mm and length 180 mm with a nut. Shear bolts are installed in holes drilled in the slab shortly before testing. The holes were drilled perpendicular to the slab plane using 16 mm diamond coring bits. The shear bolts were arranged in concentric rows parallel to the perimeter of the column.

Figure 3 shows the slab dimensions and reinforcement details. The slab has 1700 mmx1700 m and thickness 150 mm with a circular column has 250 mm diameter. Figure 3 shows the typical dimensions and reinforcement details of slab Sc [27].
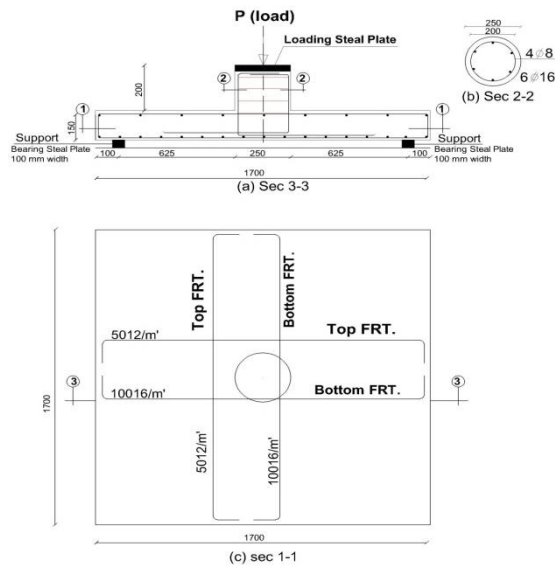
Fig. 3 Typical dimensions and reinforcement details of slab Sc [27].

3.2 Comparison between the experimental and numerical results

Figure 4 shows a comparison of the experimental and the predicted load-deflection curves, revealing excellent responses to the numerical model's accuracy at various response stages. The ultimate load, P_u, deflection at ultimate load, Δu and secant stiffness, S.S which defined as the ratio of the ultimate load to the corresponding displacement were estimated. Table 2 shows comparison between the numerical and the experimental results of slab Sc.
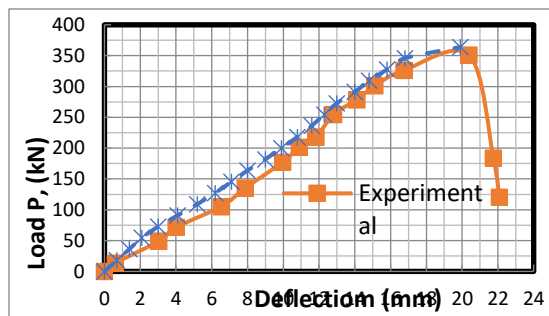
Fig. 4 Experimental and numerical load-deflection curve for slab Sc [27].

**Table 2 Comparison between the numerical and the experimental results of slab Sc [27].**

Comparison	Experimental [27]	Numerical [FE]	Exp. [27]/Num. [FE]

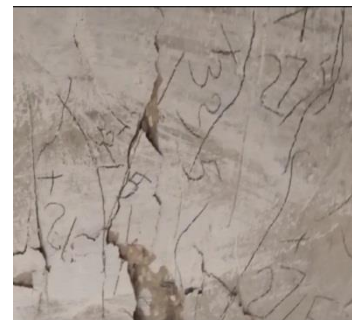|			
Ultimate load, (Pᵤ), kN	351.01	364	0.96
Deflection at ultimate load, (Δᵤ) mm	20.386	19.92	1.023
Secant stiffness (S.S), kN/ mm	17.22	18.27	0.94

The following conclusions were reached after comparing the numerical and the experimental results as shown in Fig. 4 and Table 3:

1. The finite element predictions have been close to the experimental results at the ultimate level.

2. The ratio $[(Pu\ exp/P_{uFE})]$ is 0.96. The ratio $[(\Delta_{uEXP}\ /\ \Delta_{uFE})]$ is 1.023 and the secant stiffness ratio is $(S.S_{(EXP.)}\ /S.S_{(FE))}) = 0.95$.

Early flexure cracks for Sc appeared at the middle of the slab span and became more spread as the load increased as shown in Fig.5. Figure 5 shows a very good agreement between the experimental and the numerical cracks pattern.
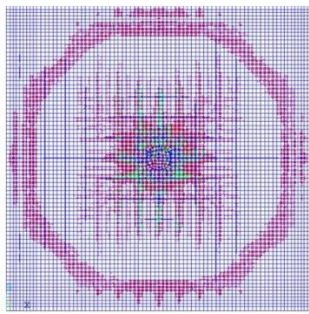
(a) **Predicted cracks pattern.**   (b) **Experimental cracks pattern.**
Fig. 5. Cracks pattern of experimental and the predicted model for slab.

4. PARAMETRIC NUMERICAL STUDY

4.1 Details of the studied slabs

Ten groups are described in Table 3 and analyzed by ANSYS programV.19. Figure 6 shows the geometry and reinforcement details of the parametric studied slabs. All slabs 2000 mm x 2000 mm, slab thickness 200 mm, $f_{cu} = 25$ MPa and $f_y = 350$ MPa with a column circular diameter 400 mm ($A_s = 8\Phi16$). S1 was the first control slab (reference slab for 24 slabs divided into 8 groups as shown in Table 3) with shear studs (bolts) diameter 8 mm, with spacing (0.5 t_s) 100 mm, one row with distance 200 mm (t_s) from column face and main steel ratio/μ_{max} (μ/μ_{max}) = 0.3 and compression steel ratio/μ_{max} (μ/μ_{max}) = 0.2 without drop panel. Slab S26 was the second control slab (reference slab for 6 slabs divided into 2 groups as shown in Table 3) without drop panel and shear studs.

Table 3 Details of the studied slabs.

Group	Slab Symbol	f_{cu} (MPa)	f_y (MPa)	Slab Thick-ness (mm)	Shear Studs (Stirrups) Diamet-er	Shear Studs (Stirrups) Spacing/ t slab	Shear Studs (Stirrups) Distances/t slab	μ / μ_{max}	$\mu` / \mu_{max}$	Drop Panel Thickness /t slab	Drop Panel Diameter/t slab	Notes
Control Specimen	FS1C	25	350	20	8	0.5	1	0.4	0.2	0	0	Control Specimen
Group (1) C	FS2C	30	350	20	8	0.5	1	0.4	0.2	0	0	Effect of f_{cu}
	FS3C	35	350	20	8	0.5	1	0.4	0.2	0	0	
	FS4C	40	350	20	8	0.5	1	0.4	0.2	0	0	
Group (2) C	FS5C	25	240	20	8	0.5	1	0.4	0.2	0	0	Effect of f_y
	FS6C	25	400	20	8	0.5	1	0.4	0.2	0	0	
	FS7C	25	420	20	8	0.5	1	0.4	0.2	0	0	
Group (3) C	FS8C	25	350	22	8	0.5	1	0.4	0.2	0	0	Effect of the Slab Thickness
	FS9C	25	350	24	8	0.5	1	0.4	0.2	0	0	
	FS10C	25	350	26	8	0.5	1	0.4	0.2	0	0	
Group (4) C	FS11C	25	350	20	6	0.5	1	0.4	0.2	0	0	Effect of Shear Studs (Stirrups) Diameter
	FS12C	25	350	20	10	0.5	1	0.4	0.2	0	0	
	FS13C	25	350	20	12	0.5	1	0.4	0.2	0	0	
Group (5) C	FS14C	25	350	20	8	0.75	1	0.4	0.2	0	0	Effect of Shear Studs (Stirrups) Spacing / t slab
	FS15C	25	350	20	8	1	1	0.4	0.2	0	0	
	FS16C	25	350	20	8	1.25	1	0.4	0.2	0	0	
Group (6) C	FS17C	25	350	20	8	0.5	0.5	0.4	0.2	0	0	Effect of Shear Studs (Stirrups) Distances/t slab
	FS18C	25	350	20	8	0.5	1.5	0.4	0.2	0	0	
	FS19C	25	350	20	8	0.5	2	0.4	0.2	0	0	
Group (7) C	FS20C	25	350	20	8	0.5	1	0.3	0.2	0	0	Effect of

	FS21C	25	350	20	8	0.5	1	0.5	0.2	0	0	Main Steel Ratio/μ_{max}
	Fs22C	25	350	20	8	0.5	1	0.6	0.2	0	0	
Group (8) C	FS23C	25	350	20	8	0.5	1	0.4	0.15	0	0	Effect of Top Steel Ratio/μ_{max}
	FS24C	25	350	20	8	0.5	1	0.4	0.25	0	0	
	FS25C	25	350	20	8	0.5	1	0.4	0. 3	0	0	
Control Specimen	FS26C	25	350	20	8	0.5	1	0.4	0.2	1	5	Control Specimen
Group (9) C	FS27C	25	350	20	8	0.5	1	0.4	0.2	1.25	5	Effect of Drop Thickness /t_{slab}
	FS28C	25	350	20	8	0.5	1	0.4	0.2	1.5	5	
	FS29C	25	350	20	8	0.5	1	0.4	0.2	2	5	
Group (10) C	FS30C	25	350	20	8	0.5	1	0.4	0.2	1	4	Effect of Drop Panel Diameter /t_{slab}
	FS31C	25	350	20	8	0.5	1	0.4	0.2	1	6	
	FS32C	25	350	20	8	0.5	1	0.4	0.2	1	8	
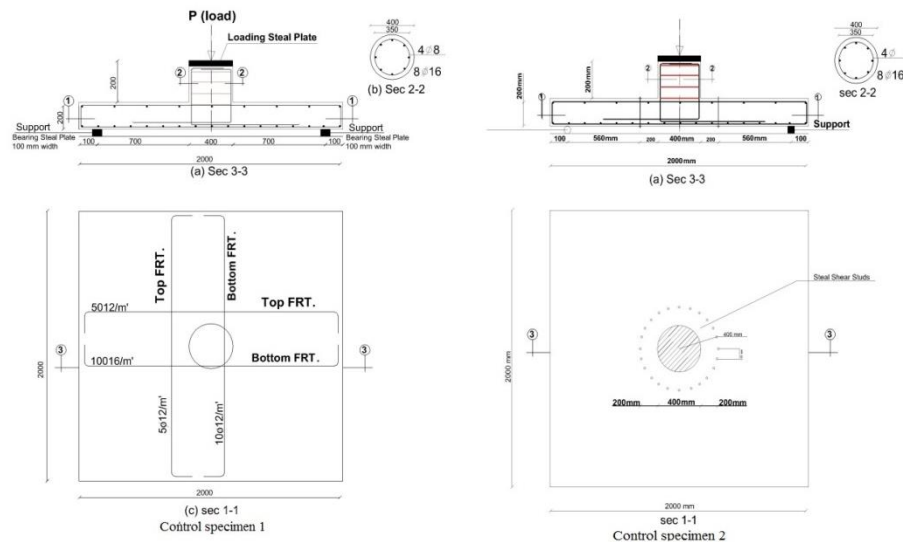
Fig.6 Geometry and reinforcement details of the parametric studied slabs.

4.2 Analysis of the numerical results

The load-deflection curves showed the behavior of the slabs by displaying a variety of response parameters, including ultimate load, deflection, and secant stiffness. Figure 7 and Table 4 shows the effect of some parameters affecting the punching shear behavior.

**Table 4 Numerical results of the studied slabs.**

Slab No.	Numerical Ultimate Load, (P_u) (kN)	Deflection at Ultimate Load (Δ_u) (mm)	Secant Stiffness (S.S) (kN/mm)	$P_u / P_{u\ S1}$ %	$\Delta_u / \Delta_{u\ S1}$ %	S.S/S.S $_{S1}$ %
S1	1056	74.84	14.11	100	100	100
S2	1188	69.12	17.19	112.5	92.36	121.83
S3	1276	66.09	19.31	120.83	88.30	136.85
S4	1364	63.39	21.52	129.17	84.70	152.51
S5	968	80.12	12.08	91.68	107.06	85.61
S6	1144	65.05	17.59	108.33	86.92	124.66
S7	1188	60.84	19.53	112.50	81.29	138.41
S8	1188	70.12	16.94	112.5	93.69	120.05
S9	1320	66.13	19.96	125	88.36	141.45
S10	1452	63.84	22.74	137.5	85.30	161.16
S11	968	77.85	12.43	91.66	104.02	88.09
S12	1144	70.61	16.20	108.33	94.34	114.81
S13	1232	64.91	18.98	116.66	86.73	134.51
S14	968	77.17	12.54	91.66	103.11	93.85
S15	880	78.93	11.15	83.33	105.46	79.02
S16	792	80.63	9.82	75	107.73	69.59
S17	792	70.10	11.30	75	93.66	80.08
S18	1188	70.61	16.82	112.5	94.34	110.20
S19	1364	71.59	19.05	129.16	95.65	135.01
S20	968	83.63	11.57	91.66	111.74	81.99
S21	1144	64.03	17.87	108.33	85.55	126.62
S22	1232	55.09	22.38	116.66	73.61	158.61
S23	924	83.56	11.06	87.50	111.65	78.37
S24	1100	65.96	16.67	104.16	88.13	118.19
S25	1188	57.17	20.78	112.50	76.39	147.27
Slab No.	Numerical Ultimate Load, (P_u) (kN)	Deflection at Ultimate Load (Δ_u) (mm)	Secant Stiffness (S.S) (kN/mm)	$P_u / P_{u\ S26}$ %	$\Delta_u / \Delta_{u\ S26}$ %	S.S/S.S $_{S26}$ %
S26	720	55.10	13.07	100	100	100
S27	1125	67.13	16.76	156.25	121.83	128.23
S28	1395	70.31	19.84	193.75	127.58	151.17
S29	1800	78.51	22.93	250	142.48	175.43

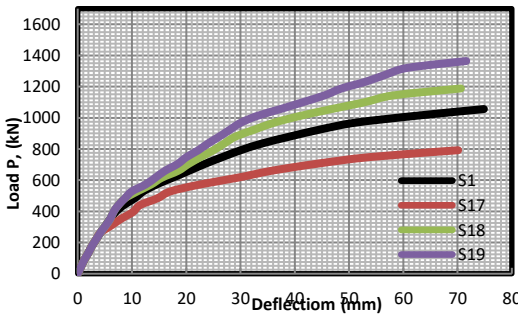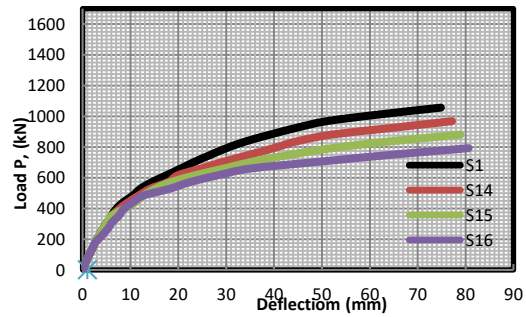| S30 | 945 | 58.18 | 16.24 | 131.25 | 105.58 | 124.25 |
| S31 | 1350 | 65.01 | 20.77 | 187.5 | 117.98 | 158.91 |
| S32 | 1530 | 69.42 | 22.04 | 212.5 | 125.98 | 168.63 |
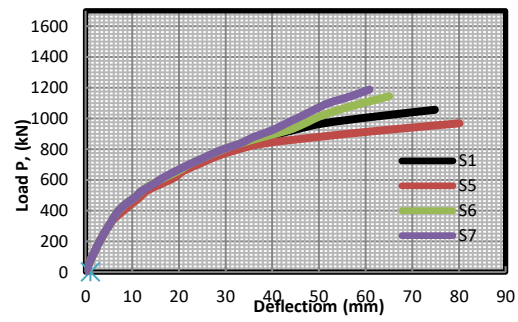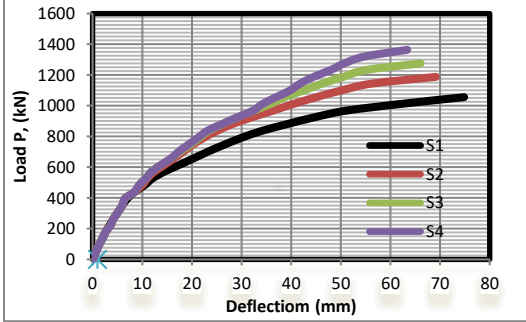
(a) Effect of Concrete Compressive Strength (f$_{cu}$)

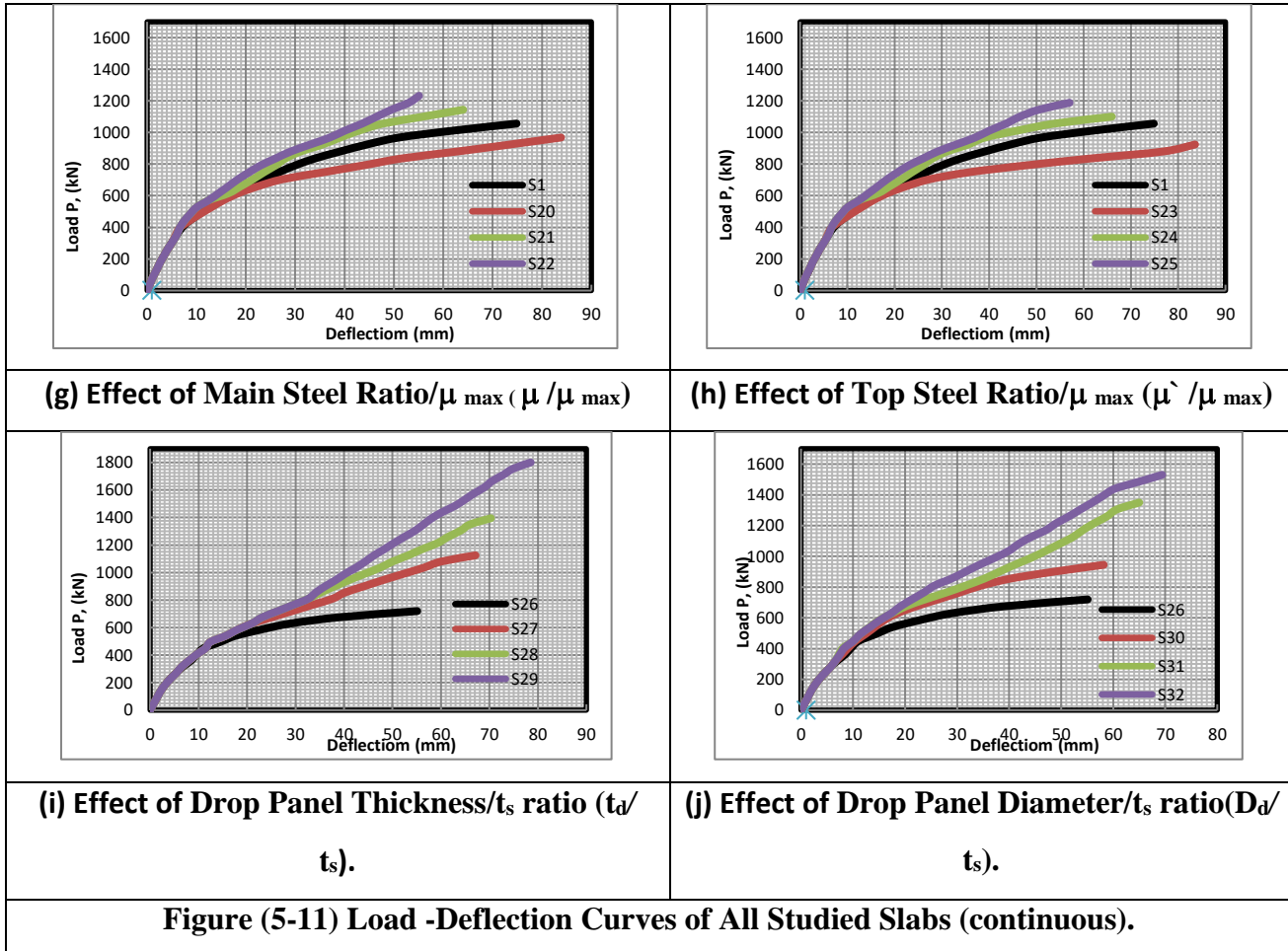**(b) Effect of Reinforcement Yield Strength (f$_y$)**
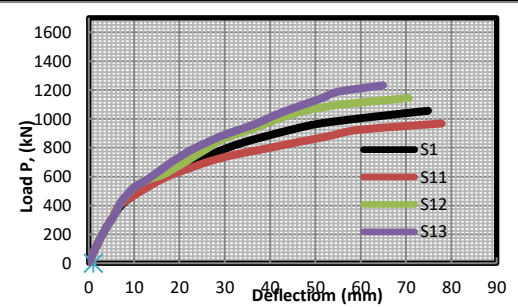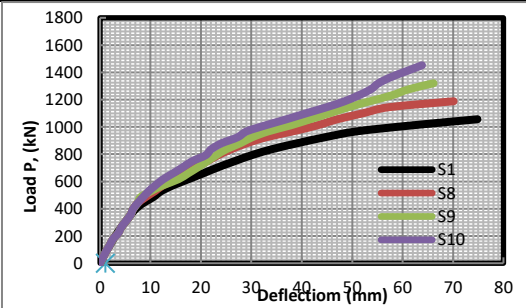
(c) Effect of Slab Thickness (t$_s$)

(d) Effect of Shear Studs Diameter (D$_b$)

(e) Effect of Shear Studs Spacing /t$_s$ ratio (S$_b$/t$_s$)

(f) Effect of Shear Studs Distances/t$_s$ atio (D/t$_s$)

(g) Effect of Main Steel Ratio/μ $_{max}$ (μ /μ $_{max}$)

(h) Effect of Top Steel Ratio/μ $_{max}$ (μ` /μ $_{max}$)

(i) Effect of Drop Panel Thickness/t_s ratio (t_d/ t_s).

(j) Effect of Drop Panel Diameter/t_s ratio(D_d/ t_s).

Figure (5-11) Load -Deflection Curves of All Studied Slabs (continuous).

4.3 Effect of concrete compressive strength (f_{cu})

Increasing concrete strength has a noticeable effect on the ultimate load. Figure 7.a and Table 4 indicted that increasing concrete strength higher secant stiffness. Also, as the concrete strength increased, higher ultimate loads reached with a noticeable small decease in deformation at the same load levels. Four slabs have the concrete compressive strength (f_{cu}) 25, 30, 35 and 40 MPa for slabs S1, S2, S3 and S4 respectively. Table 4 shows the ultimate load of slabs S2, S3 and S4, is larger than of slab S1 (reference slab) by 12.5%, 20.83% and 29.75%, respectively. In addition to the secant stiffness of slabs S2, S3 and S4, is larger than that of slab S1 by 21.83%, 36.85%, and 52.51%, respectively, although the corresponding deflections are 7.64%, 11.7%, and 15.3 % respectively lower than slab S1(reference slab). It can be noted that, the increase of the concrete compressive strength, the increase in the ultimate load and the secant stiffness, and decrease in the deflection.

4.4 Effect of reinforcement yield strength (f_y)

Three slabs are modeled and analyzed using ANSYS V19 to study the effect of reinforcement yield strength (f_y). The reinforcement yield strength (f_y) was taken

240, 400 and 420 MPa for slabs S5, S6 and S7, respectively compared to the control slab S1 (f_y = 350 MPa). As shown in Fig. 7.b, the load deflection curves are approximately the same for all slabs of group 2 at the beginning, while it varied according to the reinforcement yield strength (f_y) near the ultimate load. Based on Table 4, the ultimate load of slab S5 is less than that of slab S1 by 8.32% but slabs S6 and S7 has larger ultimate load than of that of slab S1 by 8.33% and 12.50%, respectively. In addition to the ultimate deflection of slab S5 is larger than of that of slab S1 by 7.06% but S6 and S7 is less than of that slab S1 by 13.08 %, and 18.71% respectively, although the corresponding secant stiffness of slab S5 is less than of slab S1 by 7.63% but S6 and S7 is larger than of slab S1 by 20.69 %, and 31.5%, respectively. It is clear that, the higher the reinforcement yield strength f_y, the small higher the ultimate load, secant stiffness and the lower the deflection.

4.5 Effect of slab thickness (t_s)

Figure 7.c shows the effect of increase slab thickness (t_s) on the ultimate load, secant stiffness and the deflection using three slabs S8, S9 and S10 compared to S1(reference slab). It can be noted that, an increase in both the ultimate load and secant stiffness while a decrease in deflection has been occurred as shown in Table 4.

4.6 Effect of shear studs (stirrups) diameter (Db)

From Table 4 the ultimate load and secant stiffness of slab S11 is less than that of slab S1 by (8.34 % and 11.91%) but S12 and S13 is larger than that of slab S1 by (8.33% and 14.81%) and (16.66% and 34.51) respectively. In addition to the ultimate deflection of slab S11 is larger than that of slab S1 by 7.06 % while slabs S12 and S13 has ultimate deflection less than that of slab S1 by13.08%, and 18.71% respectively. From Fig. 7.d it can be noted that the decrease of (D_b) decrease the ultimate load and secant stiffness and increasing deflection and vice versa.

4.7 Effect of shear studs (stirrups) spacing /t_s ratio (S_b/t_s)

Four slabs S1, S14, S15 and S16 has (S_b/t_s) 0.5, 0.75, 1 and 1.25 respectively. Increasing shear studs spacing (S_b) has a noticeable effect on the three slabs S14, S15 and S16, where both the ultimate load and secant stiffness decreased with an increase in the deflection as shown in Table 4 and Fig 7.e. The ultimate load and secant stiffness of slabs S14, S15 and S16 are less than that of slab S1 by (8.34% and 6.15%), (16.67% and 20.98%) and (25% and30.41%) respectively, with an increase in deflection by 3.11%, 5.46% and 7.73% respectively compared to S1 (reference slab).

4.8 Effect of shear studs (stirrups) distances/t_s ratio (D/t_s)

Group 6, study the effect of distance of shear studs (bolts) row from column face (D) where taken ratio (D/ t_s) 1.0, 0.50, 1.5 and 2 for slabs S1, S17, S18 and S19 respectively where S1 is the reference slab. Table 4 shows an increase in both the ultimate load and secant stiffness at increase (D) and vice versa while the deflection very decreased when increase or decrease (D). The ultimate load and secant stiffness of slab S17 is less than of slab S1 by (25% and 19.92%) but S18 and S19 is larger than of that of slab S1 by (12.5% and 10.20%) and (29.16% and 35.01) respectively. In addition to the ultimate deflection of slab S17, S18 and S19 is very small less than that of slab S1 by 6.34%, 5.66% and 4.35% respectively.

4.9 Effect of main steel ratio/μ_{max} (μ /μ_{max})

Table 4 and Fig 7.g showed that increasing the main steel ratio/μ_{max} increasing the ultimate load decrease the deflection leads to large secant stiffness while, the ultimate load and secant stiffness decreased and large deflection due to decreasing main steel ratio/μ_{max}. Increased and decreasing proportions ultimate load and secant stiffness, reduction and increasing ratios deflection for three slabs S20, S21 and S22 compared to S1 control specimen showed in Table 4. The ultimate deflection of slab S20 is larger than of slab S1 by 11.74% but S21 and S22 has ultimate deflection less than of that of slab S1 by14.45%, and 26.39% respectively.

4.10 Effect of compression steel ratio/μ_{max} ($\overline{\mu}$ /μ_{max})

Three slabs S23, S24 and S25 compared to S1 control specimen showed in Table 4 to study effect top steel ratio/μ_{max} on ultimate deflection, ultimate load and secant stiffness. It can be noted that a small increase in the ultimate load with big decrease in deflection led to large secant stiffness at increasing top steel ratio/□max. the ultimate load and secant stiffness of slab S23 is less than of slab S1 by (12.5% and 11.63%) respectively, while S24 and S25 is larger than of slab S1 by (4.16% and 18.19%) and (12.5% and 47.27%) respectively. In addition to the ultimate deflection of slabS5 larger than of slab S1 by 11.65% but S6 and S7 is less than of slab S1 by11.87%, and 23.61% respectively.

4.11 Effect of drop thickness/t_s ratio (t_d/ t_s)

Three slabs to study the effect of drop panel thickness/t_s ratio was taken as 0.25, 0.5 and 1.0 for slabs S27, S28 and S29 respectively compared to slab S26 (reference slab) without drop panel as shown in Table 3. Table 4 shows the ultimate load and the secant stiffness of slabs S27, S28 and S29 which are larger than of slab S26 (reference slab) by (56.25%, and 28.23%), (93.75% and 51.17%) and (150% and 75.43%) respectively. In addition to the ultimate deflections of slabs S27, S28 and S29 are larger than that of slab S26 by 7.64%, 11.7%, and 15.3 % respectively. From Fig. 7.i it can be notated that the increase of drop panel thickness/t_s ratio increase the ultimate load and decrease the deflection.

4.12 Effect of drop panel diameter/t_s ratio (D_d/ t_s)

Three slabs are used to study the effect of drop panel diameter/t_s ratio. The drop panel diameter/t_s ratio was taken 3, 5 and 6 for slabs S30, S31 and S32, respectively compared to the control slab S26 (D_d/t_s = 4) as shown in Table 4. Based on Table 4, the ultimate load of slabs S30, S31 and S32 are larger than that of slab S26 (reference slab) by 31.25%, 87.50% and 112.5%, respectively, with small increase in the ultimate deflections compared to slab S26 by 05.58%, 17.98%, and 25.98% respectively. Increasing the secant stiffness of slabs S30, S31 and S32 are larger than of slab S26 by 24.25%, 58.91% and 68.63%, respectively. From Fig 7.j it can be noted that the effect of drop panel diameter/t_s ratio has large increase in the ultimate load and has small increase in deflection.

5. Comparison of the numerical results and that calculated from Egyptian code 203-2017 [1] and ACI318-19 code [2]

The numerical results were compared with those calculated from the ECP 203-2017 [1] and ACI 318-19 [2] to verify the results as shown in Table 5.

5.1. Comparison of the numerical results and that calculated from Egyptian code 203-2017 [1]

Table 5 illustrates the comparison between the numerical ultimate load and the ultimate load calculated from Egyptian code 203-2017 [1]. The mean of the ratio of the numerical ultimate load and that calculated using Egyptian code 203-2017 [1] is 119%, the standard deviation is 13% and coefficient of variation 11% for the twenty-four-slab used in the parametric study (S1 to S24), while these values for the last six slabs used in the parametric study (S25 to S32) are 106%, 15% and 14% respectively. This comparison reveals agreement between the numerical results and those calculated using the Egyptian code 203-2017 [1].

5.2. Comparison of the numerical results and that calculated from ACI 318-19 code [2]

Good agreement between ACI 318-19 code [2] results and the nonlinear finite elements analysis was achieved. Table 5 shows the ratio between the numerical and ACI 318-19 code [2]; P_u Num /P_u ACI [2]. The mean of this ratio for the twenty-four-slab used in the parametric study (S1 to S24), the standard deviation and coefficient of variation are 111% 11% and 10% respectively, while these values for the last six slabs used in the parametric study (S25 to S32) are 116%, 15% and 13% respectively.

Table 5 Comparison of P_u using Egyptian code 203-2017 [1] and ACI 318-19 code [2] and the numerical results.

Slab No.	NLFEA result	Codes results		NLFEA / Codes		Codes
	Ultimate load $P_{u\ Num.}$ (kN)	$P_{u\ Egy..[1]}$ (kN)	$P_{u\ ACI[2]}$ (kN)	$P_{u\ Num}$ / P_u Egy.[1]	$P_{u\ Num}$ / P_u A[2]CI	$P_{u\ Egy.[1]}$ / P_u ACI[2]
1	1056	875.156	928.91	1.21	1.14	0.94
2	1188	941.6232	1017.57	1.26	1.17	0.92
3	1276	1034.622	1099.10	1.23	1.16	0.83
4	1364	1131.732	1174.99	1.20	1.16	0.75
Mean				1.23	1.16	0.83
S.D				0.03	0.006	0.08
C.O.V				0.02	0.005	0.10
5	968	875.156	928.91	1.07	1.01	0.94
6	1144	875.156	928.91	1.31	1.23	0.94
7	1188	875.156	928.91	1.36	1.28	0.94
Mean				1.25	1.17	0.94
S.D				0.15	0.14	0
C.O.V				0.12	0.12	0
8	1188	992.240	1053.19	1.20	1.13	0.94
9	1320	1113.293	1181.68	1.24	1.12	0.94
10	1452	1238.316	1314.38	1.17	1.10	0.94
Mean				1.21	1.11	0.94
S.D				0.03	0.15	0
C.O.V				0.03	0.01	0
11	968	875.156	928.91	1.11	1.04	0.94
12	1144	875.156	928.91	1.31	1.23	0.94
13	1232	875.156	928.91	1.41	1.33	0.94
Mean				1.27	1.2	0.94
S.D				0.16	0.15	0
C.O.V				0.12	0.12	0
14	968	875.156	928.91	1.11	1.04	0.94
15	880	875.156	928.91	1.01	0.95	0.94
16	792	875.156	928.91	0.91	0.86	0.94
Mean				1.01	0.95	0.94
S.D				0.1	0.09	0
C.O.V				0.99	0.095	0
17	792	696.553	739.34	1.13	1.07	0.94
18	1188	1051.949	1118.49	1.13	1.06	0.94
19	1364	1142.381	1308.06	1.19	1.04	0.87
Mean				1.15	1.06	0.92
S.D				0.03	0.015	0.04
C.O.V				0.03	0.014	0.044
20	968	875.156	928.91	1.11	1.04	0.94

21	1100	875.156	928.91	1.26	1.18	0.94
22	1232	875.156	928.91	1.40	1.32	0.94
Mean				1.26	1.18	0.94
S.D				0.14	0.14	0
C.O.V				0.11	0.12	0
23	924	875.156	928.91	1.05	0.99	0.94
24	1100	875.156	928.91	1.26	1.18	0.94
25	1188	875.156	928.91	1.36	1.28	0.94
Mean				1.22	1.15	0.94
S.D				0.16	0.15	0
C.O.V				0.13	0.13	0
Mean (total)				1.19	1.11	0.92
S.D (total)				0.13	0.11	0.04
C.O.V (total)				0.11	0.10	0.043
26	720	517.94928	483.79	1.39	1.49	1.07
27	1125	1118.25448	1044.51	1.01	1.08	1.07
28	1395	1361.35328	1235.06	1.02	1.13	1.10
29	1800	1847.55088	1537.39	0.97	1.17	1.20
Mean				1.0	1.13	1.12
S.D				0,03	0.045	0.07
C.O.V				0.03	0.04	0.06
30	945	890.03928	831.34	1.06	1.14	1.07
31	1350	1346.46968	1257.68	1.00	1.07	1.07
32	1530	1574.68488	1470.84	0.97	1.04	1.07
Mean				1.01	1.08	1.07
S.D				0.04	0.05	0
C.O.V				0.04	0.047	0
Mean (total)				1.06	1.16	1.09
S.D (total)				0.15	0.15	0.05
C.O.V (total)				0.14	0.13	0.04

6. CONCLUSIONS

The finite element (FE) analysis software program (ANSYS V. 19) was used to create the models and investigate the effects of some parameters on punching shear behavior of reinforced concrete flat slabs. Verification model was carried out to simulated a slab tested experimental by the first author. The numerical results compared with the experimental results. The results show that the numerical results matched with the experimental results and good agreement was archived. After that, some variables which included the effect of concrete compressive strength, reinforcing steel yield strength, slab thickness, shear studs diameter, shear studs spacing, shear studs distances from column face, main steel ratio/μ_{max}, top steel ratio/μ_{max}, drop thickness and drop diameter were studied. The numerical results were compared with the analytical results calculated from

ECP 203-2017 [1] and ACI 318-19 [2] and the following are the main conclusions that can be drawn from the numerical and analytical results:

1. Finite element structural modeling simulated the experimental results up to good extent.

2. The higher the concrete compressive strength and slab thickness, the higher the ultimate load, secant stiffness and the lower the corresponding deflection.

3. The load deflection curves due to the of effect of the reinforcement yield strength are approximately the same at the beginning, while it varied according to the reinforcement ratio.

4. The higher the reinforcement yield strength, shear studs diameter, main steel, compression steel, the higher the ultimate load, secant stiffness and the lower the deflection at ultimate load.
5. The lower the shear studs spacing, the lower the ultimate load, secant stiffness and the higher the deflection at ultimate load.

6. The higher the shear studs distances from column face, the higher the ultimate load and secant stiffness while decreasing shear studs distances from column face, the lower the ultimate load, secant stiffness and the lower the deflection in both cases at ultimate load.

7. The higher drop thickness and drop panel diameter, the higher the ultimate load, secant stiffness and the lower the corresponding deflection

8. The mean and standard deviation demonstrate a good agreement between the numerical results and the analytical ones calculated from ECP 203-2017 [1] and ACI 318-19 [2].

9. The most results calculated from both ECP 203-2017 [1] and ACI [2] are less than that related to the numerical results this means that both Egyptian and ACI codes are conservative.

10. The results show that ACI 318-19 code [2] is more conservative than ECP 203-2017 [1].
11. ECP 203-2017 [1] and ACI [2] code provision should be revised to add the effect of reinforcement yield strength, shear studies (diameter, spacing) and flexural steel ratio (main and compression) on calculation punching shear capacity.

7. REFERENCES

[1] Egyptian Code of Practice for Design and Construction of Reinforced Concrete Structures ECP-203, Housing and Building Research Center, Ministry of Building and Construction, Giza, Egypt, 2017, Chapter 6, pp. 113-122.
[2] ACI Committee 318-19, Building Code Required for Reinforced Concrete, (ACI 318-19) and Commentary (ACI 318R-19), American Concrete Institute, Farmington Hills, Mich,2019, Chapter 22, 4011-4020.

[3] Rasha, T.S.M., "Effect of flexural and shear reinforcement on the punching behavior of reinforced concrete flat slabs", Alexandria Engineering Journal, Vol. 56, 2017.

[4] Nasr, Z.H., and Ahmed, M. A., "Punching shear behavior of reinforced concrete using steel fibers in the mix", Housing and Building National Research, Vol. 14, pp.272-281, 2018.

[5] Santhi, A.S., "Experimental study on behavior of flat slab under different support conditions", International Journal of Pure and Applied Mathematics, Vol. 119, (12), 2018.

[6] Jae, I.J. and Su, M. K., ´ "Punching shear behavior of shear reinforced slab–column connection with varying flexural reinforcement", International Journal of Concrete Structures and Materials, 2019.

[7] Hazem, M.F., and Elbakry, S. M.A., "Punching strengthening of two-way slabs using external steel plates", Alexandria Engineering Journal, Vol.54, pp.1207-1218, 2015.

[8] Ismail, G., Abdel-Karem, A., Debeiky, A., and Makhlouf, M. "Strengthening and repair of reinforced concrete slab-column connection subjected to punching shear using (CFRP - GFRP - steel) stirrups", ICSSD, Fourth International Conference on Structural Stability and Dynamics, India, 2012.

[9] Khaleel, G.I., Shaaban, I.G., Elsayed, K.M., and Makhlouf, M.H., "Strengthening of reinforced concrete slab-column connection subjected to punching shear with FRP systems", International Conference on Civil and Architecture Engineering, Barcelona, Span, 2013 and International Journal of Engineering and Technology (IJET), August, 2013.

[10] Hasan, M. M., Mostofinejad, D., and Nakamura, H., "Strengthening of flat slabs with FRP fan for punching shear", Composite Structures, Vol. 119, pp.305-314, 2015.

[11] Hasan, M.M., Davood, M., Hakru, N., and Mohammad, H. M., "Strengthening of flat slabs with FRP fan for punching shear", Journal of Composite Structures, Vol. 119, pp.305-314, 2014.

[12] Eid, F. M., "New methods for resisting punching shear stress in reinforced concrete flat slabs", Journal of Current Engineering and Technology, Vol.8, No.2, 2018.

[13] Padmanabham, K., "Punching shear improvement of flat slabs using steel fibers and shear studs", International Journal of Civil Engineering and Technology (IJCIET), Vol. 10, Issue 11, November 2019.

[14] Mikcallef, K., Sagaseta, J., Fernandez, M. and Ruiz, A.M., "Assessing punching shear failure in reinforced concrete flat slabs subjected to localized impact loading", International Journal of Impact Engineering, 71, pp.17-33, 2014.

[15] Lips, S., Fernandez, M.R. and Muttoni, A., "Experimental investigation on punching strength and deformation capacity of shear-reinforced slabs", ACI Structural Journal,109(1): 889–900, 2012.

[16] Joaquim, A.O., Barros, B.N., Moraes, N., Guilherme, S.S.A., and Cristina, M.V.F., "Assessment of the effectiveness of steel fiber reinforcement for the punching resistance of flat slabs by experimental research and design approach", Computers Part B, 78, pp. 8-25, 2015.

[17] Robbert, K., Albin, K., and Thomas, K., "Punching shear strengthening of flat slabs using prestressed carbon fiber-reinforced polymer straps", Engineering Structures, 76, pp. 283-294, 2014.

[18] Hamed, S. A., "Repair of R/C flat plates failing in punching by vertical studs", Alexandria Engineering Journal, 2015.

[19] W. Salim and W. M. Sebastian "Plasticity Model for Predicting Punching Shear Strengths of Reinforced Concrete Slabs ", ACI Structural Journal, November-December 2002.

[20] Theodorakopoulos, D.D. and Swamy, N., "Analytical model to predict punching shear strength of FRP-reinforced concrete flat slabs", ACI Structural Journal, Vol. 24, pp. 509-520, 2002.

[21] Eder, M. A., Vollum, R.L., Elghazouli, A.Y., and Abdel-Fattah, T., "Modeling and experimental assessment of punching shear in flat slabs with spear heads", Engineering Structures ,32, pp. 3911-3924, 2010.

[22] Mikcallef, K., Sagaseta, J., Fernandez, R.M., and Muttoni, A., "Assessing punching shear failure in reinforced concrete flat slabs subjected to localized impact loading", International Journal of Impact Engineering, 71, pp. 17-33, 2014.

[23] Aikaterini, S.G., and Maria, A. P., "Finite element analysis of punching shear of concrete slabs using damaged plasticity model in ABAQUS", Engineering Structures, 98, pp. 38-48, 2015.

[24] Aikaterini, S.G., and Maria A. P., "Finite element analysis of punching shear of concrete slabs using damaged plasticity model in ABAQUS", Engineering Structures, 98, pp.38-48, 2015.

[25] Malena, B. M., and Eugen, B., "Composite model for predicting the punching resistance of R-UHPFRC-RC composite slabs", Engineering Structures, 117, pp.603-616, 2016.

[26] ANSYS Inc., Release 19.0, Documentation, Theory References, 2013.

[27] Hanna, F.H.H.," External strengthening of reinforced concrete flat slabs to resist punching using different techniques", Ph.D. (under Discussion), Faculty of Engineering, Matarya, Helwan University, Civil Engineering Department, Structure, Egypt, 2021.